Direct evidence of the anisotropy of magnetization in rare-earth metals and rare-earth/Fe_2 alloys

L. Benito,[1,2,*] K. Dumesnil,[3] and R. C. C. Ward[4]

[1]*Cavendish Laboratory, J. J. Thomson Avenue, University of Cambridge, Cambridge CB3 0HE, United Kingdom*
[2]*Department of Condensed Matter Physics, University of Zaragoza, 50009 Zaragoza, Spain*
[3]*Institut Jean Lamour (UMR CNRS 7198), Université de Lorraine, Vandoeuvre les Nancy F-54500, France*
[4]*Oxford Physics, Clarendon Laboratory, Parks Road, University of Oxford, Oxford OX1 3PU, United Kingdom*

(Received 13 September 2010; revised manuscript received 19 July 2014; published 11 August 2014)

We report on the genuine origin of the anisotropy of the magnetization M in rare-earth (RE) metals and RE-based alloys. Taking Ho-based layered nanostructures as testing ground, we prove that the anisotropy of **M** is substantial despite that the sixfold magnetic anisotropy constant K_6^6 vanishes, which contradicts the established wisdom [E. R. Callen and H. B. Callen, J. Phys. Chem. Solids **16**, 310 (1960)]. Furthermore, we show that the symmetric anisotropic contributions to M and K_6^6 vary with temperature distinctively from one another, which indicates that both anisotropic effects are unrelated and stem from dissimilar microscopic sources. Our findings are discussed according to the theory [R. J. Elliott and M. F. Thorpe, J. Appl. Phys. **39**, 802 (1968)] that predicts the emergence of symmetric anisotropic indirect-exchange terms under the presence of orbital moments. We show evidence that the anisotropy of M is caused by the indirect-exchange coupling among localized $4f$ magnetic moments mediated by spin-orbit coupled conduction electrons, which ultimately generates a spatially nonuniform spin polarization that replicates the lattice symmetry.

DOI: 10.1103/PhysRevB.90.054407 PACS number(s): 75.30.Gw, 75.50.Cc, 75.70.Cn

I. INTRODUCTION

The magnetic anisotropy energy (MAE) describes the tendency of the magnetic moments to lie along a particular set of lattice directions [1]. Its microscopic origin resides in the spin-orbit [2] coupling (SOC) through which the spin's arrangement feels the crystal-electric-field generated by the surrounding metallic ions. Closely linked to the magnetic anisotropy [2] is the anisotropy of the magnetization [3,4], which promotes the alignment of spins within a narrow cone along the easy axis (EA) while spreading them over a wider cone along the hard axis (HA). This fact leads to a smaller value of saturation magnetization M along the HA compared to the EA. While such a difference is negligible in most of bulk $3d$ ferromagnetic transition metals [5] (TM), for instance, $\sim$0.1% in Co [4], the anisotropy of M can become substantial in materials with large orbital moments [6]. However, there exists a stream of research [7], which predicts that, in the presence of nonzero orbital angular moments, the exchange interaction among neighboring magnetic moments is likely to depart from a simple Heisenberg-*like* type, comprising not only isotropic but also symmetric anisotropic terms [8,9]. This may lead to a genuine origin of the anisotropy of M, although its conclusive demonstration is proven elusive so far.

Rare-earth (RE) metals present the strongest SOC [10], making of them key metallic species in technological materials [11,12]. Contrary to $3d$ ferromagnetic TM, the saturation M attains different values along the high-symmetry lattice directions in heavy RE metals [13–16], RE-TM alloys [17], and RE-based compounds [18,19]. According to prior predictions [7–9], this observation might suggest an inherent anisotropy of the magnetization. However, this fact has been routinely explained on the grounds of the lack of saturation along the HA [4], mainly supported by the high MAE [10] values measured in RE metals.

The anisotropy of **M** in lanthanides is yet an unresolved fundamental aspect in magnetism of localized electrons, subject to a longstanding dispute [20,21]. Spin-wave [22] excitation phenomena and analysis of exotic magnetic structures [23,24] provide indirect, solid evidence, which unambiguously point to the existence of anisotropic indirect-exchange terms. However, in regard to the anisotropy of M, the established claim [4] stands unchallenged mainly because of the lack of direct evidence. Therefore, shedding light on this issue, by establishing whether the anisotropy of **M** is a genuine effect and disentangling its microscopic origin, is a fundamental theme to address with potentially far-reaching implications in magnetism, whose interest expands beyond RE-based materials [25].

In this paper, we experimentally demonstrate that the anisotropy of **M** is a genuine effect in RE metals and, by extent, in RE-based alloys and compounds. We show solid evidence that the anisotropy of M is caused by the indirect-exchange coupling between the $4f$ magnetic moments mediated by spin-orbit coupled conduction electrons, which generates a spatially nonuniform spin polarization that replicates the lattice periodicity.

In zero-field, bulk Ho orders magnetically below $T_N = 132$ K into a helical structure [26] in which the localized $4f$ magnetic moments are rigidly confined to the basal plane (BP) of the hexagonal-close-packed (HCP) structure by a huge uniaxial magnetic anisotropy [27], $K_2 \approx 2 \times 10^8$ erg/cm^3, so that the magnetic moments form a ferromagnetic (FM) sheet, wherein the direction of the magnetic moments in adjacent sheets rotates a fixed angle from one plane to the next along the c axis. At T_N, the modulation wave vector that describes the periodic structure is $\mathbf{Q} \approx (2/7)\mathbf{c}^*$, which reduces on cooling down to $T_C = 18$ K at which **Q** becomes equal to $(1/6)\mathbf{c}^*$, and the magnetic moments tilt out of the basal plane to form a

*luisbenito.phys@gmail.com

conelike structure. The H-T magnetic phase diagram (MPD) in bulk Ho [28] shows a complex set of magnetic structures, among which a helical-antiferromagnetic (H-AFM), a fan and forced FM state, and intermediate phases like helifan and exotic spin-slip [29] phases are found. Basically, under an increasing in-plane applied magnetic field, **H**, the zero-field H-AFM structure transforms abruptly into a fan phase [14], which under further increase in **H** gradually turns into a forced FM state. In Ho/Lu SLs, as occurs in strained-alike Dy/Lu SLs [30], the epitaxial compression strain shifts T_C towards high temperatures [31]; we find that $T_C = 26$ K for the Ho_{35}/Lu_{15}. Equally, the H-T MPD in the Ho/Lu SLs [32] is greatly simplified when compared to bulk Ho [28], and it is also observed that the critical fields that mark the transitions from the H-AFM phase to the fan one and from this latter to the forced FM state are notably reduced as the Ho layer thickness T_{Ho} gets thinner, so that M-H curves saturate at lower H, reflecting on the downsizing of K_6^6 with T_{Ho} [33].

II. EXPERIMENTAL METHODS AND SAMPLE DETAILS

The samples investigated are a Ho thin film 500-nm thick and a $[Ho_{35\pm2}Lu_{15\pm1}]_{50}$ superlattice (SL), where 35 ± 2 and 15 ± 1 refer to the number of monolayers (MLs) for the Ho and Lu layers, respectively, and 50 refers to the number of Ho/Lu bilayer repetitions in the SL structure. These samples are fully representative of a much wider investigation conducted in a set of RE-based (RE = Ho and Dy) thin films and SLs. All Ho-based nanostructures were grown using a molecular beam epitaxy technique in a UHV chamber, a Balzers UMS630 facility, with a base pressure better than 2×10^{-10} mbar onto "epi-polished" $(11\bar{2}0)$-oriented heated Al_2O_3 substrates, following the deposition techniques described elsewhere [34,35]. These growing techniques assure that the deposited RE layers grow with the **c** axis normal to the substrate plane and are epitaxially aligned, forming high-quality single crystals.

High-resolution x-ray diffraction [35,36] measurements show that the average coherent length along the growth direction is of ∼200 nm, the mosaic width is ∼0.15°, and the interface width is around about 2–4 MLs. In addition, the atomic spacing along growth direction in the Ho/Lu SLs is larger when compared to that in bulk Ho [10], which suggests an in-plane compression strain, consistent with similar findings in strain-alike Dy/Lu [30] SLs.

Magnetic torque experiments and M-H curves were performed in an *in-home* made high-resolution vector vibrating sample magnetometer [37] (VVSM), which records the spatial components of the magnetization, allowing us to determine **M**, unlike conventional hysteresis loops [38] collected for different **H** orientations, in which only the projection of **M** onto **H** is determined. The sample is rotated with respect to **H**, so that the rotation axis is collinear to the hexagonal axis of the sample, whereas **H** is applied in the BP of the HCP structure, as outlined in Fig. 1(a). The VVSM provides the longitudinal, $M_{\parallel}(\varphi)$ and transversal $M_{\perp}(\varphi)$ components of **M**, with respect to **H** in the rotation plane, as a function of the rotation angle, φ. **M** and **H** make angles ϕ (crystal angle) and φ, respectively, with the in-plane easy direction, and α is the angle that makes

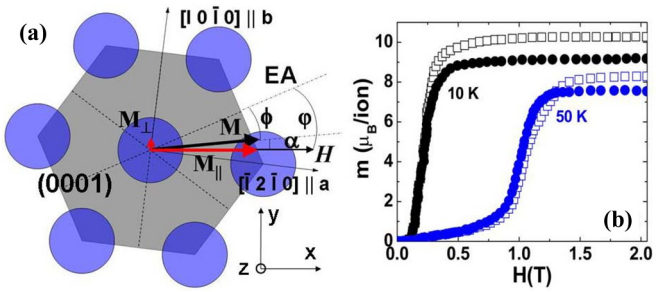

FIG. 1. (Color online) (a) Sketch of the sample rotation within (0001) plane in a rare-earth system, showing the angular relationships between **M**, **H** and the easy axis, EA. The vector set $\{x,y,z\}$ refers to a Cartesian system. (b) $m_{\parallel}(H)$ for **H**‖**b** axis (empty squares) and **H**‖**a** axis (full circles) collected in a Ho_{35}/Lu_{15} superlattice. (See text for further details.)

M with **H**. The magnetic torque, $L_k(\phi)$, is then given by

$$L_k(\phi) = -BM\sin\alpha = -HM_{\perp}(\varphi), \tag{1}$$

where it was considered that the demagnetizing factor $N_D = 0$. We directly determine $M_{\perp}(\varphi)$ and we gain access to $M_{\perp}(\phi)$ by using the relationship $\phi = \alpha - \varphi$, where α is also obtained as $\alpha(\varphi) = \arctan(M_{\perp}(\varphi)/M_{\parallel}(\varphi))$. Torque experiments were conducted at temperatures within the range $T = 5-100$ K and for a field range of $\mu_0 H = 1.5-2$ T [we notice that for $T \leqslant 30$ K the field range was wider, i.e., $\mu_0 H = 1-2$ T]. $M_{\parallel}$ and $M_{\perp}$ are collected in φ steps, $\Delta\varphi = 1.8°$, so that the time interval, Δt, between two consecutive φ steps is $\Delta t = 10$ s. This Δt is large enough to guarantee that the detection electronics provides a largely stable read-out and that $M_{\parallel}$ and $M_{\perp}$ are the magnetization components at the equilibrium. Notice that Δt is orders of magnitude larger than the dynamical response time featured by magnetic systems, typically smaller than a microsecond [39]. A complete set $\{M_{\parallel}(\varphi), M_{\perp}\varphi)\}_{\varphi=0-360°}$, for a fixed value of temperature and applied magnetic field, is completed in around about 1 hour, and the experimental time scale, t_{exp}, in our torque experiments is $t_{exp} \sim 330$ s. Lastly, we notice that the VVSM instrument also enables to determine M_z, i.e., the component of M perpendicular to the sample's plane. During the execution of the torque experiments, we checked that M_z remains below the sensitivity limit, i.e., $M_z(\varphi) < 10^{-7}$ emu, which means that M_z is totally negligible when compared to the in-plane components.

III. RESULTS AND DISCUSSION

We have chosen Ho-based layered nanostructures to investigate the anisotropy of M, firstly, because as occurs in bulk Ho [26], the magnetic moments in Ho/Lu [36] SLs and Ho thin films lie in the BP of the HCP lattice structure, i.e., the rotation plane, so that the analysis of vector magnetization measurements are subject to a minimum uncertainty [notice that $N_D = 0$ in this configuration]. Secondly and, more importantly, Ho possesses the highest MAE values [10] within the RE metal series and holds a complex, but rich magnetic phenomena [40,41], which makes of it the ideal candidate to explore and challenge the establishment [4] on the origin of the anisotropy of the magnetization.

A. Coherent rotation of M in torque experiments

Firstly, it is instrumental to the analysis that follows to establish whether throughout the torque experiment **M** rotates uniformly (coherently). Because this concept is quite often mistaken for that dealing with the coherent (incoherent) switching of M during the record of hysteresis loops [38,42], a detailed clarification is much needed. If proven that **M** rotates coherently, then $\mathbf{M}(\phi)$ can be unequivocally obtained as

$$M(\phi) = (M_{\parallel}^2(\phi) + M_{\perp}^2(\phi))^{1/2}. \quad (2)$$

At a fixed temperature, H is applied along the EA in Ho/Lu SL, this is $\mathbf{H}\|\mathbf{b}$, and then H is raised up to the maximum value, i.e., $\mu_0 H = 2$ T, so that the magnetic moments in the Ho/Lu SL are fully aligned along **H** direction [see Fig. 1(b)]. As occurs in bulk Ho, the saturation M in the SL also attains different values when **H** is along the **b** and the **a** directions. At a glance, the M-H curve collected at $T = 10$ K suggests the onset of a fully aligned state for $\mu_0 H > 0.4$ T. At $T = 50$ K, the onset of the fan phase is clearly pointed out by a slope change in M-H curve, as an intermediate phase between a distorter H-AFM phase, for $\mu_0 H < 0.7$ T, and a forced FM state, for $\mu_0 H > 1.4$ T.

We notice that the way in which a torque experiment is conducted differs from that exploring the coherent (incoherent) switching of M during a hysteresis loop [42]. In the former, H is firstly aligned along the EA, then increased up to a value large enough to induce a forced FM state, and hold it. Subsequently, the sample is rotated against **H**, so that only **H** orientation changes with respect to the lattice directions and **M**, but its strength is kept at a constant value.

Let us commence by assuming that the anisotropy of M is a mere artifact. We will explore whether the above hypothesis is probable. Recalling that M is confined to the c plane [27] by a huge uniaxial anisotropy, the anisotropy field in bulk Ho is $\mu_0 H_k (\approx 2K_2/M) \simeq 13$ T (taking $M = 3 \times 10^3$ kA/m). A similar order of magnitude for H_k may be expected [43] in RE-based SLs. Considering the above and bearing in mind that both in-plane components of M are experimentally recorded, the only possible mechanism by which the anisotropy of M might occur is as a result of a nonuniform(incoherent) rotation process of M, as outlined in Fig. 2. In this way, starting from a fully aligned spin structure in the Ho/Lu SL induced by applying a magnetic field of 2 T along the b axis, the sample remains in a single-domain (SD) state as long as **H** is away from the HA [see Fig. 2(a)]. At $T = 10$ K, K_6^6 is large enough [33], so that M stays close to the EA despite that the sample is rotated against **H** and towards the next EA. This is well reflected in the linear increase shown by α with φ until H is close to the HA [see Fig. 3(a)], which produces a moderate increase in the magnetic anisotropy plus Zeeman energy, E_{kZ}, for small ϕ values around the EA, typically for $\phi < 7^\circ$ [see Fig. 3(b)]. As the sample is rotated further and **H** approaches the HA, only then **M** moves away from one EA towards the next-nearest EA. This event is well featured by the sawtoothlike variation of $\alpha(\varphi)$ [see Fig. 3(a)], where it is seen that α oscillates between $\pm 20^\circ$ and M realignment takes place over a narrow window in φ, typically around about 10.8°, coinciding with H being close to and passing over the HA. This entails a substantial increase in E_{kZ} for ϕ values in-between two consecutive EAs [see Fig. 3(b)].

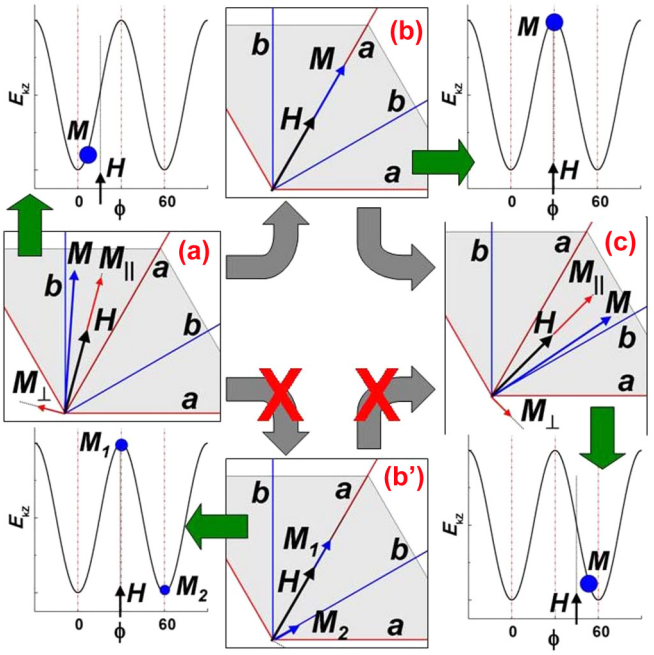

FIG. 2. (Color online) Longitudinal, $M_{\parallel}$, and transversal, $M_{\perp}$, components of the magnetization M with respect to the applied magnetic field, H(=2 T), in the c plane of the hexagonal structure, so that **b** is the easy axis (EA) and **a** is the hard axis (HA) for M. The sequence (a)⇒(b)⇒(c) corresponds to a coherent rotation of **M** when the sample is rotated against **H** towards the next-nearer EA. The sequence (a)⇒(b')⇒(c) corresponds to an incoherent rotation of M. (See text for further details.)

It seems apparent that a nonuniform rotation of M would minimize the increase in anisotropy energy experienced by the system when H approaches the HA and M moves from one EA to the next-nearest EA [see Figs. 2(a), 2(b'), and 2(c)], compared to the scenario in which **M** uniformly rotates towards the next EA [see Figs. 2(a), 2(b), and 2(c)]. An incoherent rotation of M implies that the SD state with magnetization, M, splits into a multidomain (MD) state, let us assume two domains for simplicity [see Figs. 2(a) and 2(b')],

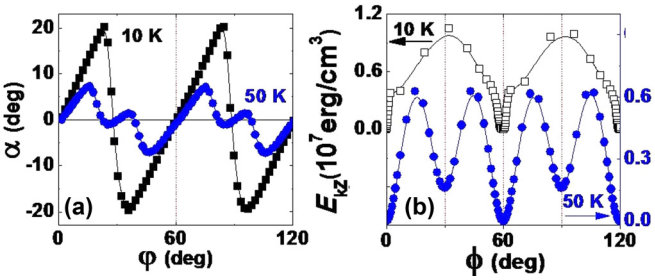

FIG. 3. (Color online) (a) $\alpha(\varphi)$ at $T = 10$ K (full squares) and $T = 50$ K (empty circles) for $\mu_0 H = 2$ T. (b) Experimental magnetic anisotropy plus Zeeman energy, $E_{kZ} = K_6^6 \cos 6\phi - HM \cos\alpha(\phi)$, at $T = 10$ and 50 K for $\mu_0 H = 2$ T. Plots have been shifted to adjust $E_{kZ}(\phi_{\min}) = 0$. All data have been collected in a Ho_{35}/Lu_{15} superlattice (for further details see text).

so that $M = M_1 + M_2$ and $M_1 > M_2$, where M_1 and M_2 are the magnetizations of each domain. The newly nucleated domain with magnetization $\mathbf{M}_2$ would be oriented along the next-nearest EA. As the sample is further rotated and H moves away from the HA towards the next EA, then both domains, $\mathbf{M}_1$ and $\mathbf{M}_2$, would merge, forming an SD state as outlined in Figs. 2(b') and 2(c). The onset of an MD state would account for the diminishing of M around the HA and the modulated anisotropy of M would be originated in the repeated switching between a single- and a multidomain state when H passes over an EA and HA, respectively. Before entering into further analysis of the energy balance in E_{kZ}, formation of domain walls and so on, as a result of the nonuniform rotation, we must firstly establish whether the onset of an MD state is a likely event to occur during the course of a torque experiment.

In order for an MD state to form [see Fig. 2(b')], a fraction of the total volume of the *macroscopic* sample, in this case a Ho/Lu SL, corresponding to the magnetization M_2, must go through the energy barrier ΔE_{kZ}. In the classical limit, the thermally activated barrier hopping with relaxation time τ is given by the Néel-Arrhenius equation

$$\tau = \tau_0 \exp(V \Delta E_{kZ}/k_B T), \tag{3}$$

where V is the volume of sample hopping the barrier, K_B is the Boltzmann constant, T is the absolute temperature, and τ_0 is the hopping attempt time, which is typically of the order of 10^{-9}–10^{-13} s. Using the values displayed in Fig. 3(b) to calculate the order of magnitude of ΔE_{kZ}, typically $\sim 10^6$ erg/cm^3, and assuming that the volume of the sample hopping the barrier is a small fraction of the sample's volume, for instance a $\sim$1% for illustrative purposes, that is, $V \sim 10^{-7}$ cm^3. We notice that in order to reproduce a typical 10% change in M, the fraction of M that should go through ΔE_{kZ} should be much larger. Making use of Eq. (3) (notice that $V \Delta E_{kZ}/k_B \approx 10^{15}$ K), it is straightforward to estimate that $\tau \gg t_{\text{exp}}$ at any temperature, and the same is true for a larger V. On the other hand, at temperatures approaching the absolute zero, we find that the macroscopic quantum tunneling rate is given by the following expression [44]:

$$\Gamma \simeq \Gamma_0 \exp\left(-2S\sqrt{K_6^6/K_2}\right), \tag{4}$$

where typically $\Gamma_0 \approx 10^{11}$ Hz, K_6^6 is the effective sixfold anisotropy constant [33], and s is the number of individual magnetic moments contained in the volume of material that accounts for the observed change in M. As above, we assume a 1% variation in M for illustrative purposes. Now, inserting $K_6^6/K_2 \sim 10^{-2}$ and $s \sim 10^{15}$ into Eq. (4), results in that $\Gamma^{-1} \gg t_{\text{exp}}$. We hereby conclude that the probability to form an MD state during the course of a torque experiment, conducted in a highly anisotropic *macroscopic* sample, is completely negligible at any temperature and, therefore, $\mathbf{M}$ rotates coherently in the **c** plane throughout the torque experiment. This means that $M(\phi)$ can be safely obtained from Eq. (2).

B. Anisotropy of the magnetization and MAE

The VVSM [37] instrument enables to obtain the model-independent $M_\parallel$ and $M_\perp$, and using Eq. (2), M is obtained, as shown in Fig. 4 for a Ho thin film 500-nm thick. This approach

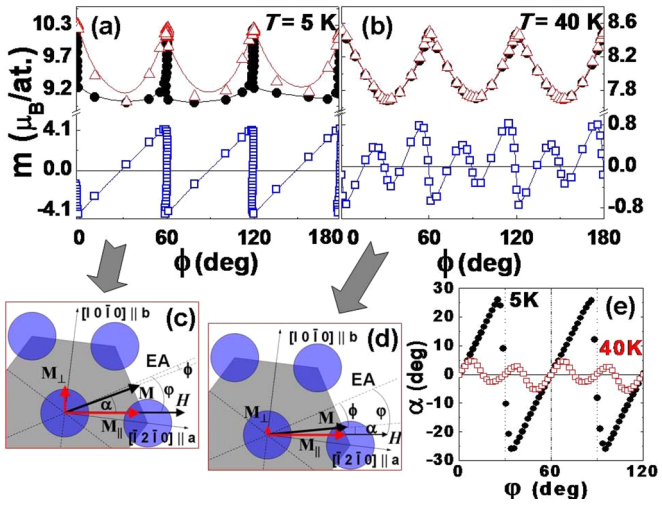

FIG. 4. (Color online) (Top) Longitudinal (full black circles) and transversal (empty blue squares) components of the magnetic moment (empty red triangle) with respect to the applied magnetic field H vs the crystal angle ϕ in the basal plane of the HCP structure for a (0001)-oriented Ho thin film 500-nm thick, so that $\mathbf{H} \perp$ c and $\mu_0 H = 2$ T, (a) at $T = 5$ K and (b) at $T = 40$ K. (Bottom) Sketch illustrating the magnetization M arrangement for the top panel plots: (c) $T = 5$ K large anisotropy field H_k and (d) $T = 40$ K low H_k. (e) $\alpha(\varphi)$ for the top panel plots at $T = 5$ K (full circles) and $T = 40$ K (empty squares). (See text for further details.)

is far more informative than the conventional collection of M-H loops [45] at fixed φ, which ultimately provides no information at all about $M_\perp$. In RE metals, the in-plane anisotropy field is such as, $H_k \propto K_6^6$, and given that K_6^6 is large at very low temperatures [33], then $H_k/H < 1$ for laboratory magnetic fields. This reflects in that, at $T = 5$ K, $\mathbf{M}$ stays close to the EAs throughout the torque experiment, so that $\mathbf{M}$ only starts moving away from one EA towards the next-nearest EA as H is closely approaching the HA. Thus $M_\parallel$ and $M_\perp$ curves show bunching data around the EAs, i.e., experimental data are unevenly distributed on ϕ [see Figs. 4(a) and 4(c)]. Consistently, $\alpha(\varphi)$ features a characteristic sawtoothlike dependence, oscillating between $\pm 26^\circ$ [see Fig. 4(e)]. At $T = 40$ K, $H_k/H \ll 1$ given that K_6^6 decays quickly with temperature [33], which reflects in that $\mathbf{M}$ follows $\mathbf{H}$ closely throughout the torque experiment [see Figs. 4(b) and 4(d)]. Distinctively, α features a sinusoidal-like dependence on φ in this occasion and its oscillation range is narrower, i.e., $\pm 5^\circ$ [see Fig. 4(e)]. In this scenario, the $M_\parallel$ and $M_\perp$ curves show data evenly distributed on ϕ [see Fig. 4(b)]. As can be seen from inspecting $M_\perp$ in Figs. 4(a) and 4(b), as temperature increases, a 12-fold symmetry arises. Previous studies [40] showed that in Ho-based systems the MAE is better modeled by including hexagonal and 12-fold magnetic anisotropy constants and that the competing single- and two-ion magnetoelastic contributions to this latter give rise to its inhomogeneous T dependence [41]. Ultimately, this unusual behavior originates a change in the symmetry shown by $M_\perp$ as temperature increases.

Inspecting $E_{kZ}(\phi)$ allows us to gain further insight concerning the dynamical behavior of $\mathbf{M}$ over the course of the

torque experiment, as illustrated in the case of the Ho/Lu SL [see Fig. 3(b)]. At $T = 10$ K, where K_6^6 is large enough, the anisotropy energy dominates over the Zeeman term and, hence, **M** stays close to the EAs for most of the torque experiment in order to minimize E_{kZ}. Notice that E_{kZ} presents a "bunching" effect of the plotted data around the EAs. However, as temperature rises, see graph at $T = 50$ K, K_6^6 rapidly decreases and, as a result, the Zeeman term dominates over the magnetic anisotropy one, so that **M** follows **H** closely throughout the torque experiment. Consistently, at $T = 50$ K, E_{kZ} curve displays data evenly distributed on ϕ and α features a typical sinusoidal-like dependence on ϕ [see Fig. 3(a)].

Not surprisingly, the Ho thin film replicates the behavior of the bulk Ho [14]. In this way, we find that M exhibits a remarkable anisotropy at $T = 5$ K [see Fig. 4(a)]. If we define the oscillation amplitude as half the difference between the magnetic moment measured along the b axis, m_b, and the a axis, m_a, this is $\Delta m = (m_b - m_a)/2$, then we find that $\Delta m \simeq 0.55\mu_B$ at $T = 5$ K. However, what surprises the most is that, at $T = 40$ K, the **b** and the **a** directions become both EAs, but $\Delta m \simeq 0.4\mu_B$ [see Fig. 4(b)]. This means that Δm is still very much comparable to that at $T = 5$ K, despite that the sixfold magnetic anisotropy energy is visibly smaller at higher temperature, as deduced from comparing the transversal component of the magnetic moment [or $M_\perp$, if applied] at both temperatures. Importantly, this crucial observation raises serious concerns about the validity of the established origin [4] of the anisotropy of M.

As mentioned earlier, the anisotropy of M also appears in RE-Fe_2 alloys [17] and RE-based [18,19] compounds. We briefly illustrate this aspect in a (110)-oriented $TbFe_2$ thin film 130-nm thick [see Fig. 5(a)]. We note that $TbFe_2$ alloy is an important technological material, since it presents the largest magnetoelastic [46] coupling at room temperature. M-H loops [47] collected along the high-symmetry cubic directions show a fully aligned ferrimagnetic state for $\mu_0 H > 1.3$–1.5 T, wherein the saturation $M_\parallel$ reaches different values when H is aligned along the set of directions {111} and {110}, in good agreement with Fig. 5(a). Furthermore,

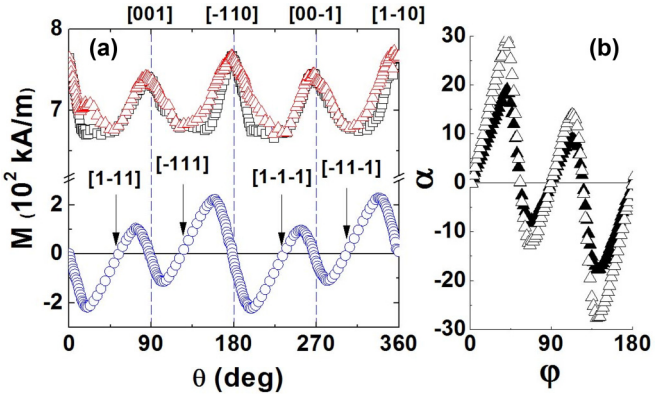

FIG. 5. (Color online) (a) Longitudinal (black squares) and transversal (blue circles) components of the magnetization (red triangle) with respect to the applied magnetic field H vs the crystal angle θ in the rotation plane (110) for a (110)-oriented $TbFe_2$ thick thin film 130 nm at room temperature and for $\mu_0 H = 2$ T. (See text for further details.)

vector magnetization measurements reveal a strain-induced modification of the MAE in $TbFe_2$ thin films grown onto $(11\bar{2}0)$-oriented Al_2O_3/(110)Nb/NbFe-φ structure [48], so that the directions $[\bar{1}10]$ and $[1\bar{1}0]$ are the EAs in the thin film, then followed by [001] and $[00\bar{1}]$ and, lastly, we find that the hardest set of directions is {111}. Interestingly, the calculated α that reproduces the observed anisotropy of M, shows a variation between $\pm 30^\circ$ [see Fig. 5(b)], which exceeds by far the experimental one, which shows a narrower oscillation, i.e., $\pm 18^\circ$.

We estimate that the shape anisotropy field in the thin film is $\mu_0 H_{sh}[= M(N_{in} - N_{out})] \simeq 1$ T, and this tends to confine M in-plane, where we have taken $M = 770$ kA/m, $N_{in} \simeq 0$, and $N_{out} \simeq 1$, being these latter the in- and out-of-plane demagnetization factors, respectively. Building on the discussion given in Sec. III A, if we assume in first order of approximation the magnetic anisotropy constants for the bulk alloy [49], we hereby can conclude that M rotates uniformly in the (110) plane of the $TbFe_2$ thin film. Therefore we find that the experimental ratio δ defined as $\delta = (M_{[\bar{1}10]} - M_{[1\bar{1}\bar{1}]})/M_{[1\bar{1}\bar{1}]} \approx 0.15$ cannot be explained on the grounds of the lack of saturation, since M should not show a major variation with θ, unless the anisotropy of **M** is an inherent effect to the $TbFe_2$ alloy. Additionally, $M_\parallel$ and $M_\perp$ curves show evenly distributed data [see Fig. 5], which indicates that the Zeeman term dominates ($H_k/H \ll 1$) and, as a result, **M** follows **H** closely throughout the rotation. More intriguingly, at lower temperatures and in a softer alloy, i.e., Terfenol-D thin film [17], an equivalently defined δ factor yields a striking value of around about 0.4.

Vector magnetization studies in Ho/Lu SLs unveiled a rich phenomena [40,41] on which we will build to further explore the origin of the anisotropy of **M** and test its scalability. To facilitate comparing MAE values obtained at different temperatures and H strengths, we notice that $K_6^6 \propto M_\perp^{max}$, where $M_\perp^{max}$ is the maximum value reached by $M_\perp$ around the EA. At all temperatures, M shows a sixfold oscillatory dependence on ϕ [see Figs. 6(a)–6(d)]. At $T = 10$ K, $M_\parallel$ presents sharp peaks when M crosses through EA directions, i.e., the **b** directions, which coincide with crossings through zero with negative slope for $M_\perp$ [see Fig. 2(a)]. As temperature increases, MAE quickly decreases [33] and $M_\parallel$ progressively turns into a sinusoidal-like function on ϕ, so that $M_\parallel$ and M match each other [see Figs. 6(a) and 6(c)]. Strikingly, despite that $M_\parallel$ and $M_\perp$ show a dissimilar dependence on ϕ from each other, $M(\phi)$ remains almost unchanged as temperature increases, which is an indication that the temperature scaling of $M_\perp$ and M may be somehow uncorrelated.

At $T = 50$ K, the Ho/Lu SL undergoes a field-induced easy axis reorientation [40] (EAR), so that for $\mu_0 H = 1.5$ T, $M_\perp$ predominantly shows twelvefold [41] symmetry [see Fig. 6(d)]. To be precise, the EAR has already taken place for $\mu_0 H = 1.5$ T and a Fourier analysis of $L_k(\propto M_\perp)$ unveils six- and twelvefold harmonics, so that $K_{12}^{12} \gg K_6^6$ and that $K_6^6 \simeq 0$, where K_{12}^{12} is the twelvefold magnetic anisotropy constant [41]. As shown in Fig. 6(d), $M_\perp$ crosses through zero at the **b** and **a** directions with almost identical negative slope, which means that both directions are twin EAs. Crucially, we find that the anisotropy of M is comparable to that for $\mu_0 H = 2$ T, despite that

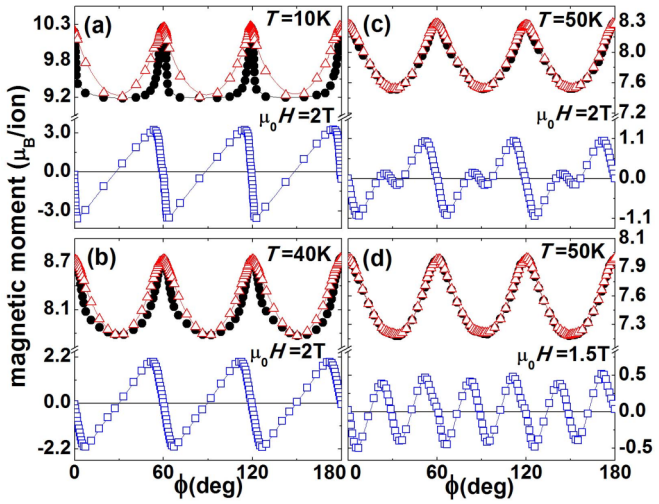

FIG. 6. (Color online) Longitudinal, $m_{\parallel}$ (circles), and transversal, $m_{\perp}$ (squares), components of the magnetic moment **m** with respect to the applied magnetic field H and $m = (m_{\parallel}^2 + m_{\perp}^2)^{1/2}$ (triangles) for $\mathbf{H}\perp\mathbf{c}$ axis, collected in a Ho_{35}/Lu_{15} superlattice. $\phi = 0$ corresponds to the **b** axis. (See text for further details.)

the sixfold magnetic anisotropy vanishes. Furthermore, we find that Δm slightly increases from 0.35 μ_B for $\mu_0 H = 1.5$ T up to 0.41 μ_B for $\mu_0 H = 2$ T, whereas K_6^6 increases with H from nearly a null value up to $8 \times 10^5 \mathrm{erg/cm^3}$ [compare Figs. 6(c) and 6(d)]. Building on the evidence here exposed, we hereby conclude that the anisotropy of M is a genuine and scalable effect.

C. Origin of the anisotropy of M: anisotropic indirect-exchange coupling mediated by spin-orbit coupled conduction electrons

According to the Russell-Sanders coupling scheme [10], the RE electrons in the unfilled $4f$ shell are described by a total spin **S** and orbital **L** momenta, which are combined into a total angular moment $\mathbf{J} = \mathbf{S} + \mathbf{L}$. The energy gap between the ground, J, and first-excited multiplet, $J + 1$, is $\Pi = \zeta_{4f}/2S$ [50], where ζ_{4f} ($\simeq$0.2 eV in the RE series) is the spin-orbit coupling constant for the $4f$ shell [51], so that for Ho^{3+} $\Pi =$ 8500 K. Importantly, this means that the magnetic moment in heavy RE^{3+} ions is given by the fundamental state. In the RE series, except for Gd ($L = 0$), the $4f$ shell presents nonzero orbital moments with pronounced multipoles, i.e., $L = 6$ in the case of Ho^{3+}.

In the metallic state, the onset of magnetic order is accomplished through the polarization of the $(6s5d)^3$ conduction electrons (CEs) by means of an indirect-exchange coupling or so-called RKKY interaction [52]. This entails that the experimental magnetic moment per RE^{+3} ion, m, is slightly in excess [10] to that theoretically predicted [51], so that m can be written as

$$m = m_{4f} + m_{sd}, \tag{5}$$

where $m_{4f} \sim \mu_B \langle \mathbf{J}_{4f} \rangle$ is the contribution of the unfilled $4f$ shell [51] ($m_{4f} = 10\mu_B$ in Ho) and m_{sd} is the magnetic moment of the spin-polarized mixed s-d character conduction bands, which in bulk Ho is estimated that amounts to $0.34\mu_B$. In an oversimplified model, the CEs are regarded as uncoupled electron-free-like and, under such a crude assumption, the k-independent band splitting is given by the spin-up $\varepsilon_{n,\mathbf{k},\uparrow}$ and spin-down $\varepsilon_{n,\mathbf{k},\downarrow}$ subbands as $\Delta = \varepsilon_{n,\mathbf{k},\uparrow} - \varepsilon_{n,\mathbf{k},\downarrow} = 2\langle J_z \rangle J_{sd,f}$, where $J_{sd,f}$ is the direct-exchange coupling between the localized $4f$ clouds and the CEs, so that m_{sd} reads as [53]

$$m_{sd} = \mu_B \mathcal{N}(\varepsilon_F)\Delta, \tag{6}$$

where $\mathcal{N}(\varepsilon_F)$ is the density of states per ion per spin state, ε_F is the Fermi energy, and we have assumed the Landé g factor, $g = 2$, for the CEs.

Neglecting orbital effects leads to an isotropic indirect-exchange coupling, which in general enables a basic understanding [20,52] of the complex magnetic phenomena in RE metals. However, there exist numerous evidences gathered from a variety of sources, among which we recall the spin-wave excitation analysis [54–58], neutron studies [59], modeling of the indirect-exchange interaction under different scenarios [60–64], and calculations of spin-wave [65] excitations, that strongly suggest the anisotropic nature of the RKKY interaction in lanthanides. In fact, the assumption of an isotropic indirect-exchange coupling is fully justified only if the radial extent of the $4f$ electronic clouds R_{4f} and the Fermi wave vector k_F are such that, $R_{4f}k_F \ll 1$, which is indeed far from being the case, given that the $4f$-electron and CE wave functions substantially overlap [51,66].

A number of studies [8,9,67,68] have investigated the possible origins of the anisotropic indirect-exchange coupling terms, which are found numerous and varied in nature [68], but otherwise restricted by symmetry [22]. The physical mechanisms leading to the appearance of anisotropic indirect-exchange terms in RE metals have been discussed in detail by Jensen *et al.* [58], who elucidated that, according to symmetry considerations, the emergence of two-ion anisotropic terms is highly likely to be caused by the indirect-exchange coupling between $4f$ magnetic moments mediated by spin-orbit coupled CEs [69].

The above claim is firmly underpinned by the following arguments. (1) Earlier calculations [61,62] set out that, under the presence of nonzero localized orbital moments, the indirect-exchange coupling between $4f$ magnetic moments, mediated by freelike uncoupled conduction electrons, gives rise to anisotropic interaction terms (derived from Coulomb forces), which amount to around about 10%–20% out of the dominant isotropic indirect-exchange term. (2) In RE metals, the conduction bands closely resemble that of $5d$ transition metals [66,70,71], where those intersecting the Fermi level possess a predominantly d-like character [72], which implies a large density of states at the ε_F, i.e., $\mathcal{N}(\varepsilon_F) = 1.8$ electrons [53] per ion per eV. (3) An estimation of the SOC constant for the d-like CEs obtained that $\zeta_d \simeq 0.03$ eV [73], which is smaller but still comparable to the calculated direct-exchange coupling in Gd [53], this is $J_{sd,f} \simeq 0.09$ eV [note that this figure must be taken as the upper limit in the RE series], and substantially larger when compared to $3d$ metals, for which $\zeta_{3d} \simeq 1$ meV [74]. (4) Unusual Andreev reflection spectroscopy data collected in Ho thin films are found characteristic of spin-mixing-like properties [75], which may reflect in the spin-orbit induced splitting [76] of the conduction bands. (5) Lastly, considering the effect that spin-orbit coupling has

upon the conduction bands is proven instrumental to gain a better understanding of the relation between electronic and magnetic properties in RE metals that otherwise would remain poorly described or simply unaccounted, i.e., the electron band structure [77] in the FM phase, the origin of the magnetic anisotropy [78] and the electronic structure [79] in Gd metal, and the mixing mechanism between acoustic magnons and optic phonons [73].

A major consequence of the relativistic effects in magnetic solids is that an electron moving in a metallic lattice through a nonuniform potential feels an effective magnetic field acting on its spin. For the CEs, this can be expressed by means of the spin-orbit Hamiltonian, which reads as, $\mathcal{H}_{\rm SO} = \sum_i \zeta_{sd}(r_i)\mathbf{l}_i \cdot \mathbf{s}_i$, where $\mathbf{l}$ and $\mathbf{s}$ are the orbital and spin moment and the sum runs over the s-d conduction-band wave functions, and $\zeta_{sd} = \frac{\hbar^2}{2m^2c^2}\frac{1}{r_i}\frac{dV(r)}{dr}$, so that $V(\mathrm{r})$ includes the periodic potentials generated by the RE^{+3} ion cores in the HCP lattice, in addition to the potential created by the diffusive electron densities themselves. The Coulomb forces [61,62], resulting from the overlapping between the localized $4f$ and diffusive $6s5d$ electron densities, will introduce interband spin-mixing terms through the SOC [69] into the electronic band structure, reflecting in the differentiated shifting exerted over the s- and d-like states in the conduction bands. As a result of the mixed action of the direct-exchange and spin-orbit couplings the conduction band will show a spatially nonuniform spin polarization, replicating the periodicity of the HCP lattice [80]. This means that $m_{sd} \equiv m_{sd}(\phi)$ in Eq. (6), so that $\mathcal{N}(\varepsilon_F)$ reads as

$$\mathcal{N}(\varepsilon_F) = \frac{1}{\Delta}\int_{\varepsilon_F-\frac{\Delta}{2}}^{\varepsilon_F+\frac{\Delta}{2}} \mathcal{N}(\varepsilon)d\varepsilon;\ \Delta \simeq 2\langle J_z\rangle \mathcal{J}^{\rm ani}_{sd,f}, \qquad (7)$$

where we define $\mathcal{J}^{\rm ani}_{sd,f}$ as the anisotropic direct-exchange coupling constant between the $4f$ electron densities and the spin-orbit coupled CEs. Its anisotropic origin resides in the singular manner in which the inseparable action of the exchange and the relativistic effects are jointly combined to polarize the spin bath in strongly correlated systems. In a simplistic, but more intuitive picture, this combined effect can be regarded as the coupled CEs moving in the $V(r)$ potential "experience" a symmetric anisotropic polarizing field acting on their spin. Thereby, $\mathcal{J}^{\rm ani}_{sd,f}$ is inherently dependent on the orientation of the localized magnetic moments with respect to the HCP lattice axes.

We find that the lowest-rank Hamiltonian that accounts for the anisotropic indirect-exchange terms [10,51] reads as

$$\mathcal{H}^{\rm ani}_{JJ} = -\frac{1}{2}\sum_{i,j}\mathcal{K}_{sd,f}(\mathbf{R}_{ij})J_{i\zeta}J_{j\zeta}\cos 6\phi_{ij}, \qquad (8)$$

where $\mathbf{R}_{ij} \equiv \mathbf{R}_i - \mathbf{R}_j$, $\mathbf{R}_{i(j)}$ is the equilibrium position for the $i(j)$th ion in the HCP lattice, ϕ_{ij} is the angle between the ζ axis, and the projection of $\mathbf{R}_{ij}$ on the BP, where the anisotropic RKKY constant, $\mathcal{K}_{sd,f}$, holds the physical information of the indirect-exchange coupling between anisotropic $4f$ magnetic moments mediated by the spin-orbit coupled CEs. Notice that in formulating $\mathcal{H}^{\rm ani}_{JJ}$ [see Eq. (8)], the angular momentum operators are referred to the (ξ,η,ζ) reference system, where $\widehat{\eta}$ is in the BP and $\widehat{\zeta} \parallel \widehat{\mathbf{u}}$, so that $\widehat{\mathbf{u}}$ is an arbitrary direction within the BP described by the polar angles $(\pi/2,\phi)$ and $\mathbf{M}\parallel \widehat{\mathbf{u}}$. In addition, the threefold symmetry presented by the c axis is also taking into account.

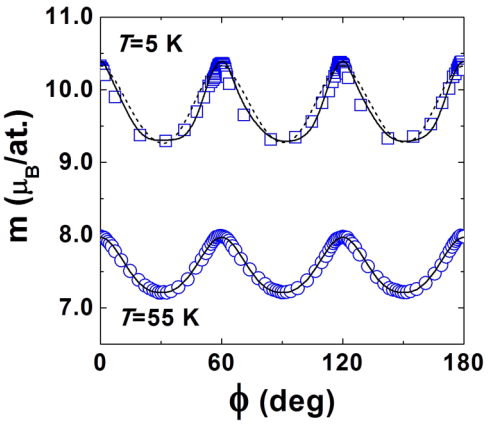

FIG. 7. (Color online) Magnetic moment $m = (m_\parallel^2 + m_\perp^2)^{1/2}$ as a function of the crystal angle ϕ in the c plane for an applied magnetic field, $\mu_0 H = 2$ T, collected in a $\mathrm{Ho}_{35}/\mathrm{Lu}_{15}$ superlattice. The lines correspond to a fit of the experimental data according to the equation $m = \sum_{k=0,6,12} m_k \cos k\varphi$, so that the continuous and dashed lines result from including harmonics with $k = 0$, 6, 12, and $k = 0$, 6, respectively. The best-fit parameters are, at $T = 5$ K, $m_0 = 9.7\mu_B$, $m_6 = 0.54\mu_B$, and $m_{12} = 0.2\mu_B$, and, at $T = 55$ K, $m_0 = 7.55\mu_B$, $m_6 = 0.38\mu_B$, and $m_{12} = 0.05\mu_B$ (see text for further details).

Producing an estimation of the nonuniform spin polarization created by the anisotropic RKKY interaction by utilizing state-of-the-art *ab initio* calculation techniques [78] is a complex task and, although it may turn out certainly illuminating, this is clearly beyond the scope of this study. Alternatively, this investigation shows conclusive evidence that m_{sd} is genuinely anisotropic and replicates the periodicity of the lattice, as seen in Fig. 7. In this way, a Fourier analysis of $m(\phi)$ reveals that the experimental data can be accurately simulated using the following equation:

$$m = m_0 + m_6\cos 6\phi, \qquad (9)$$

where according to Eq. (5), we identify $m_0 = m_{4f}$ and $m_{sd} = m_6\cos 6\phi$ [notice that in this notation $m_6 \equiv \Delta m$, defined this latter in Sec. III B]. The obtained value for m_{4f} at $T = 5$ K is $9.7\mu_B$, this is 3% smaller than the theoretical one but still within the uncertainty of the experimental error. Despite this uncertainly, the experiment seems to elucidate that the spin polarization of the CEs is mainly nonuniform, which verifies the arguments aforementioned laid down concerning the anisotropic nature of $\mathcal{J}^{\rm ani}_{sd,f}$. At $T \leqslant 10$ K, adding a second harmonic to Eq. (9) results in a fitting function that matches slightly better $m(\phi)$, as seen in Fig. 7. Now, turning to the Hartree-Fock decoupling [81] approximation to evaluate the thermal average of the two-ion angular momentum operator in Eq. (8), we obtain that [82] $\langle J_{i\zeta}J_{j\zeta}\rangle \propto [\sigma(T)]^2$, where σ is the reduced magnetization, i.e., $\sigma = M(T)/M(0)$, and therefore, $\langle \mathcal{H}^{\rm ani}_{JJ}\rangle$ shows a similar scaling with temperature to the isotropic exchange energy [51]. This isomorphism is also translated to the scaling of Δm with the temperature, so that from Eqs. (6) and (7), and bearing in mind that $\langle J_\zeta\rangle \propto \sigma$, we then conclude that $\Delta m \approx \Delta m_0\sigma(T)$.

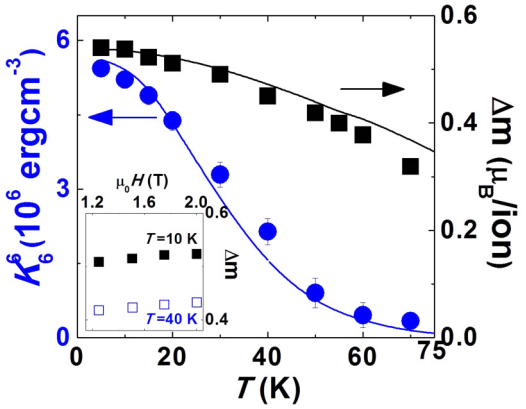

FIG. 8. (Color online) Temperature dependence of the anisotropic spin polarization, Δm (squares), and the in-plane sixfold magnetic anisotropy constant, K_6^6 (circles), determined in a Ho_{35}/Lu_{15} superlattice. The solid lines correspond to a theoretical fit of the experiment data, so that $\Delta m = \Delta m_0 \sigma(T)$ with $\Delta m_0 = 0.56\mu_B$, and $K_6^6 = K_{6,\mathrm{MCME}}^6 \widehat{I}_{13/2}[\widetilde{\sigma}] + K_{6,\mathrm{ME}}^6 \widehat{I}_{9/2}[\widetilde{\sigma}]\widehat{I}_{5/2}[\widetilde{\sigma}]$ [33], where $\widehat{I}_p[\widetilde{\sigma}]$ is the reduced hyperbolic Bessel function, $\widetilde{\sigma} \equiv \mathcal{L}^{-1}[\sigma(T)]$ is the inverse Langevin function of the reduced magnetization $\sigma(T) = M(T)/M(0)$ and the best-fit parameters are $K_{6,\mathrm{MCME}}^6 = -3.7 \times 10^6$ erg/cm^3 and $K_{6,\mathrm{ME}}^6 = 9.5 \times 10^6$ erg/cm^3, where the former is the magnetocrystalline and magnetoelastic (MCME) and the latter the pure magnetoelastic (ME) contributions to the effective sixfold magnetic anisotropy constant. Inset graph displays Δm as a function of the applied magnetic field H at representative temperatures. For further details see text.

Following well-established methods [83], we have determined the field-independent K_6^6 at different temperatures. We notice that Δm exhibits a very gentle dependence on H, for the field range $\mu_0 H = 1$–2 T and for the examined temperatures [see Fig. 8]. For that reason, we have opted for plotting Δm at the maximum applied field, i.e., $\mu_0 H = 2$ T. Bearing in mind that the temperature dependence of any physical magnitude is a distinctive fingerprint of its microscopic origin, we hereby conclude that in the light of the differentiated temperature scaling posed by K_6^6 and Δm, see Fig. 8, these possess dissimilar microscopic origins. In particular, the K_6^6 dependence on T is well-fitted by the single-ion theory [84], provided strain-induced magnetoelastic [33] contributions are included, and $\Delta m \propto \sigma(T)$, in excellent accord with the arguments given above, which indicates that its origin resides in the two-ion anisotropic indirect-exchange coupling mediated by spin-orbit coupled CEs, as earlier discussed.

IV. CONCLUSIONS

As a summary, we have laid down formal arguments, which show that in highly anisotropic magnets the magnetization rotates coherently during a torque experiment, provided the applied magnetic field is large enough to induce a FM state along the easy axis. Building on this, we have unequivocally determined **M** as a function of the crystal angle and, hereby, experimentally demonstrated the genuine origin of the spatial anisotropy of **M** in rare-earth metals, taking Ho-based layered nanostructures as testing ground. In particular, we have shown that the anisotropy of the magnetization is substantial, ≈10%, despite that the sixfold magnetic anisotropy vanishes and that the symmetric anisotropic contributions to the total magnetic moment and the K_6^6 vary with temperature distinctively from one another, which indicates that both anisotropic effects stem from dissimilar microscopic sources. Our results are consistent with the prediction [7,9] of the emergence of symmetric anisotropic indirect-exchange terms under the presence of large orbital moments. We have equally shown solid evidence that the anisotropy of M is caused by the anisotropic indirect-exchange coupling among the localized $4f$ magnetic moments mediated by spin-orbit coupled conduction electrons, which induces a spatially nonuniform spin polarization in the latter that replicates the lattice periodicity.

We stress that proving the concept of the anisotropy of the magnetization is an important step forward towards gaining a better understanding of the spin-related phenomena in RE-based materials. Thus the anisotropy of the magnetization reaches large ratios, ≈40%, in $REFe_2$ alloys [17] and appears to be a widespread phenomenon in rare-earth transition-metal (RE-TM) intermetallics, where the anisotropic nature [49] of the RE-TM is attributed to the large orbital moment of the RE sublattice and the conduction band results from the hybridization [85] of the d-like states and the $6s5d$-like ones given up by the TM and RE sublattices, respectively.

In a broader context, this study offers a novel perspective on spin-orbit related phenomena with far-reaching implications. The spin polarization in RE-based systems is likely to be proven strain dependent, given that $\mathcal{J}_{sd,f}^{\mathrm{ani}}$ is inherently a function of $\mathbf{R}_{ij}$, where changing the relative interionic distance in the metallic lattice will primarily modify the direct-exchange coupling and, therefore, the Coulomb forces between the $4f$ electron clouds and the surrounding spin-orbit coupled $6s5d$-like diffusive densities. If this strain effect is experimentally demonstrated, then this may open up the possibility to exploit the *two-ion magnetoelastic coupling* to engineer novel all-electric voltage-controlled energy-efficient hybrid devices by bringing together tailored piezoelectric/RE-based heterostructures, in which the spin transport [86] in the top layer may be tuned by the strain developed by the bottom one.

ACKNOWLEDGMENT

One of us (L.B.) acknowledges financial support from the European Commission (PEOPLE-programm) for a Marie Curie IEF contract (ref.: MEIF-CT-2006-025693).

[1] S. Chikazumi, *Physics of Magnetism* (Willey, New York 1978).
[2] J. H. van Vleck, Phys. Rev. **52**, 1178 (1937).
[3] E. R. Callen, J. Appl. Phys. **31**, S149 (1960).
[4] E. R. Callen and H. B. Callen, J. Phys. Chem. Solids **16**, 310 (1960).
[5] S. Kaya, Sci. Rep. Tohoku Univ. **17**, 639 (1928).

[6] J. M. Alameda, D. Givord, R. Lemaire, and Q. Lu, J. Appl. Phys. **52**, 2079 (1981).
[7] T. Moriya, Phys. Rev. **120**, 91 (1960).
[8] T. Kasuya and D. H. Lyons, J. Phys. Soc. Jpn. **21**, 287 (1966).
[9] R. J. Elliott and M. F. Thorpe, J. Appl. Phys. **39**, 802 (1968).
[10] *Magnetic properties of Rare Earth Metals*, edited by R. J. Elliott (Plenium, London, 1972).
[11] J. F. Herbst, Rev. Mod. Phys. **63**, 819 (1991).
[12] N. C. Koon, C. M. Williams, and B. N. Das, J. Magn. Magn. Mater. **100**, 173 (1991).
[13] D. R. Behrendt, S. Legvold, and F. H. Spedding, Phys. Rev. **109**, 1544 (1958).
[14] D. L. Strandburg, S. Legvold, and F. H. Sppeding, Phys. Rev. **127**, 2046 (1962).
[15] D. E. Hegland, S. Legvold, and F. H. Spedding, Phys. Rev. **131**, 158 (1963).
[16] H. E. Nigh, S. Legvold, and F. H. Spedding, Phys. Rev. **132**, 1092 (1963).
[17] C. de la Fuente, J. I. Arnaudas, L. Benito, M. Ciria, A. del Moral, C. Dufour and K. Dumesnil, J. Phys.: Condens. Matter **16**, 2959 (2004).
[18] D. Dufeu, E. Eyraud, and P. Lethuillier, Rev. Sci. Instrum. **71**, 458 (2000).
[19] Ya. Mudryk, N. K. Singh, V. K. Pecharsky, D. L. Schlagel, T. A. Lograsso, and K. A. Gschneidner, Jr., Phys. Rev. B **85**, 094432 (2012).
[20] P.-A. Lindgård, Phys. Rev. Lett. **36**, 385 (1976).
[21] J. Jensen, Phys. Rev. Lett. **37**, 951 (1976); P.-A. Lindgård, *ibid.* **37**, 954 (1976).
[22] J. Jensen, Physica B **86-88**, 32 (1977).
[23] R. A. Cowley and J. Jensen, J. Phys.: Condens. Matter **4**, 9673 (1992).
[24] J. Jensen and R. A. Cowley, Europhys. Lett. **21**, 705 (1993).
[25] M. Venkatesan, C. B. Fitzgerald, J. G. Lunney, and J. M. D. Coey, Phys. Rev. Lett. **93**, 177206 (2004).
[26] W. C. Koehler, J. W. Cable, M. K. Wilkinson, and E. O. Wollan, Phys. Rev. **151**, 414 (1966).
[27] J. J. Rhyne, S. Foner, E. J. McNiff, and R. Doclo, J. Appl. Phys. **39**, 892 (1968).
[28] W. C. Koehler, J. W. Cable, H. R. Child, M. K. Wilkinson, and E. O. Wollan, Phys. Rev. **158**, 450 (1967).
[29] D. Gibbs, D. E. Moncton, K. L. D'Amico, J. Bohr, and B. H. Grier Phys. Rev. Lett. **55**, 234 (1985).
[30] R. S. Beach, J. A. Borchers, A. Matheny, R. W. Erwin, M. B. Salamon, B. Everitt, K. Pettit, J. J. Rhyne, and C. P. Flynn, Phys. Rev. Lett. **70**, 3502 (1993).
[31] G. J. Tomka, P. A. J. de Groot, B. D. Rainford, M. R. Wells, R. C. C. Ward, and J. I. Arnaudas, J. Magn. Magn. Mater. **140-144**, 785 (1995).
[32] P. P. Swaddling, D. F. MacMorrow, R. A. Cowley, J. A. Simpson, M. R. Wells, R. C. C. Ward, K. N. Clausen, M. F. Collins, and W. J. L. Buyers, J. Magn. Magn. Mater. **140-144**, 783 (1995).
[33] L. Benito, J. I. Arnaudas, M. Ciria, C. de la Fuente, A. del Moral, R. C. C. Ward, and M. R. Wells, Phys. Rev. B **70**, 052403 (2004).
[34] R. C. C. Ward, M. R. Wells, C. Bryn-Jacobsen, R. A. Cowley, D. F. McMorrow, and J. A. Simpson, Thin Solid Films **275**, 137 (1996).
[35] D. F. McMorrow, P. P. Swaddling, R. A. Cowley, R. C. C. Ward, and M. R. Wells, J. Phys.: Condens. Matter **8**, 6553 (1996).
[36] P. P. Swaddling, R. A. Cowley, R. C. C. Ward, M. R. Wells, and D. F. McMorrow, Phys. Rev. B **53**, 6488 (1996).
[37] L. Benito, J. I. Arnaudas, and A. del Moral, Rev. Sci. Instrum. **77**, 025101 (2006).
[38] G. Bertotti, *Hysteresis in Magnetism* (Academic Press, 1998).
[39] A. Aharoni, *Introduction to the Theory of Ferromagnetism* (Oxford University Press, Oxford 2001).
[40] L. Benito, M. Ciria, C. de la Fuente, J. I. Arnaudas, R. C. C. Ward, and M. R. Wells, Phys. Rev. Lett. **94**, 227204 (2005).
[41] L. Benito, M. Ciria, A. Fraile, D. Fort, J. S. Abell, and J. I. Arnaudas, Phys. Rev. Lett. **98**, 267201 (2007).
[42] A. Hubert and R. Schäfer, *Magnetic Domains* (Springer-Verlag, 2000).
[43] L. Benito, R. C. C. Ward, and M. G. Blamire, Phys. Rev. B **88**, 224407 (2013).
[44] E. M. Chudnovsky and J. Tejada, *Macroscopic Quantum Tunneling of the Magnetic Moment* (Cambridge University Press, Cambridge, 1998), pp. 29–61.
[45] E. C. Stoner and E. P. Wohlfarth, Phil. Trans. Roy. Soc. A **240**, 599 (1948).
[46] A. E. Clark and H. S. Belson, Phys. Rev. B **5**, 3642 (1972).
[47] V. Oderno, Ph.D. Thesis, Institut Polytechnique de Lorraine, Nancy, France, 1996.
[48] V. Oderno, C. Dufour, K. Dumesnil, Ph. Mangin, and G. Marchal, J. Cryst. Growth **165**, 175 (1996).
[49] A. E. Clark, in *Handbook on the Physics and Chemistry of Rare Earths*, edited by K. A. Gschneider and L. Eyring, (North-Holland, Amsterdam, 1979), Vol. 2, Chap. 15.
[50] G. H. Dieke, *Spectra and Energy Levels of Rare Earth Ions in Crytals* (Wiley, New York, 1968).
[51] J. Jensen and A. R. Mackintosh, *Rare Earth Magnetism: Structures and Excitations* (Clarendon Press, Oxford, 1991), http://www.nbi.ku.dk/page40667.htm
[52] T. Kasuya, in *Magnetism*, edited by G. T. Rado and H. Suhl, (Academic Press Inc., New York 1966), Vol. IIB.
[53] R. E. Watson, A. J. Freeman and, J. O. Dimmock, Phys. Rev. **167**, 497 (1968).
[54] R. M. Nicklow, N. Wakabayashi, and M. K. Wilkinson, Phys. Rev. Lett. **27**, 334 (1971).
[55] P. A. Lindgård, and J. G. Houmann, in *Proceedings of the Durham Conference on Rare Earths and Actinides*, edited by E. W. Lee (Institute of Physics, London, 1971), p. 192.
[56] J. Jensen, J. Phys. F **4**, 1065 (1974).
[57] J. G. Houmann, M. Chappelier, A. R. Mackintosh, P. Bak, O. D. McMaster, and K. A. Gschneidner, Jr. Phys. Rev. Lett. **34**, 587 (1975).
[58] J. Jensen, J. G. Houmann, and H. B. Møller, Phys. Rev. B **12**, 303 (1975).
[59] F. Tsui, C. P. Flynn, M. B. Salamon, R. W. Erwin, J. A. Borchers, and J. J. Rhyne, Phys. Rev. B **43**, 13320 (1991).
[60] S. H. Liu, Phys. Rev. **121**, 451 (1961).
[61] T. A. Kaplan and D. H. Lyons, Phys. Rev. **129**, 2072 (1963).
[62] F. Specht, Phys. Rev. **162**, 389 (1967).
[63] P. M. Levy, Phys. Rev. **177**, 509 (1969).
[64] Y. Yafet, J. Appl. Phys. **61**, 4058 (1987).
[65] J. G. Houmann, B. D. Rainford, J. Jensen, and A. R. Makintosh, Phys. Rev. B **20**, 1105 (1979).
[66] A. J. Freeman, *Magnetic properties of Rare Earth Metals*, edited byR. J. Elliott (Plenium, London, 1972), pp. 245–333.

[67] P.-A. Lindgård and O. Danielsen, Phys. Rev. B **11**, 351 (1975).
[68] W. P. Wolf, J. Phys. Colloques **32**, C1-26 (1971).
[69] P. M. Levy, Phys. Rev. Lett. **20**, 1366 (1968); Phys. Rev. **177**, 509 (1969); Solid State Commun. **7**, 1813 (1969).
[70] A. J. Freeman, J. O. Dimmock and, R. E. Watson, Phys. Rev. Lett. **16**, 94 (1966).
[71] S. C. Keeton and T. L. Loucks, Phys. Rev. **168**, 672 (1968).
[72] J. O. Dimmock and A. J. Freeman, Phys. Rev. Lett. **13**, 750 (1964); J. O. Dimmock, A. J. Freeman, and R. E. Watson, J. Appl. Phys. **36**, 1142 (1965).
[73] S. H. Liu, Phys. Rev. Lett. **29**, 793 (1972).
[74] A. Abragam and B. Bleaney, *Electron Paramagnetic Resonance of Transition Ions* (Oxford University Press, Oxford, 1970).
[75] I. T. M. Usman, K. A. Yates, J. D. Moore, K. Morrison, V. K. Pecharsky, K. A. Gschneidner, T. Verhagen, J. Aarts, V. I. Zverev, J. W. A. Robinson, J. D. S. Witt, M. G. Blamire, and L. F. Cohen, Phys. Rev. B **83**, 144518 (2011).
[76] R. J. Elliott, Phys. Rev. **96**, 266 (1954); Y. Yafet, *Solid State Physics* (Academic Press, New York, 1963), Vol. 14.
[77] K. M. Döbrich, G. Bihlmayer, K. Starke, J. E. Prieto, K. Rossnagel, H. Koh, E. Rotenberg, S. Blügel, and G. Kaindl, Phys. Rev. B **76**, 035123 (2007); K. M. Döbrich, A. Bostwick, J. L. McChesney, K. Rossnagel, E. Rotenberg, and G. Kaindl, Phys. Rev. Lett. **104**, 246401 (2010).
[78] M. Colarieti-Tosti, S. I. Simak, R. Ahuja, L. Nordström, O. Eriksson, D. Åberg, S. Edvardsson, and M. S. S. Brooks, Phys. Rev. Lett. **91**, 157201 (2003).
[79] K. Maiti, M. C. Malagoli, A. Dallmeyer, and C. Carbone, Phys. Rev. Lett. **88**, 167205 (2002).
[80] J. Jensen and A. R. Mackintosh, *Rare Earth Magnetism: Structures and Excitations* (Clarendon Press, Oxford, 1991), p. 259.
[81] E. Callen and H. B. Callen, Phys. Rev. **139**, A455 (1965).
[82] L. Benito, J. I. Aranudas, M. Ciria, C. de la Fuente, and A. del Moral, J. Phys.: Condens. Matter **16**, 7151 (2004).
[83] L. Benito, C. Ballesteros, and R. C. C. Ward, Phys. Rev. B **89**, 134421 (2014).
[84] E. R. Callen and H. B. Callen, J. Phys. Chem. Solids **27**, 1271 (1966).
[85] M. A. Laguna-Marco, J. Chaboy, and C. Piquer, Phys. Rev. B **77**, 125132 (2008).
[86] S. N. Gordeev, J-M. L. Beaujour, G. J. Bowden, B. D. Rainford, P. A. J. de Groot, R. C. C. Ward, M. R. Wells, and A. G. M. Jansen, Phys. Rev. Lett. **87**, 186808 (2001).